Rotation rates of inactive satellites near geosynchronous earth orbit

Rita L. Cognion
Oceanit

ABSTRACT

Stabilized satellites in geosynchronous earth orbit (GEO) become drifters after they are decommissioned. In addition, each satellite begins to tumble or precess in its inactive state. As they drift around the earth, the inactive satellites provide sequential viewing opportunities---with synodic periods of months or weeks---for observation with an earth-based sensor. In order to measure their rotation rates as a function of time, we track a set of inactive satellites over several months as each comes into view over Hawaii. Images of each satellite are acquired through a small (0.4-m) optical telescope system with sampling periods of a few seconds. With temporal light curves obtained through relative, in-frame photometry on each image, we analyze both the time and frequency domains in order to determine the satellites' rotation rates.

1. INTRODUCTION

Geosynchronous earth orbit (GEO) contains many of humankind's most valuable satellite assets. It is also populated with inactive satellites and other debris that threaten the assets. Debris mitigation strategies are in development; two of these are the European Space Agency's Clean Space initiative [1,2], and the Phoenix program funded by the Defense Advanced Research Projects Agency (DARPA) [3]. Weeden, et al., [4] summarize some recent international activities in proximity operations and active debris removal.

Inactive satellites will present themselves as large, tumbling, uncooperative targets to any debris mitigation solution. To develop an effective mitigation approach, an understanding of the evolution of the satellite dynamics is needed. In this investigation, the rotation rates of a set of inactive satellites are observed in order to help characterize their dynamics as a function of time.

A decommissioned subset of the Geostationary Operational Environmental Satellite (GOES) constellation is a nearly-ideal test case for this investigation. Of the same build, but sequentially decommissioned over a period of almost ten years, each of the five satellites known as GOES 8 through 12 lies at a different point on the timeline of its evolution toward a (hypothesized) stable state. Over a period of several months, each satellite was observed as it drifted into view over Maui, and its rotation period was determined.

2. THE SATELLITES

Each of the five satellites numbered GOES 8 through GOES 12 (originally known as GOES I through M) is nearly identical in construction to the others in its block [5]. Fig. 1 shows the outline and dimensions of these satellites. Because they share a common build, and because they have been sequentially decommissioned over almost ten years, they are particularly suited to temporal investigations of inactive satellite dynamics. Table 1 lists their launch and decommission dates. More detailed information regarding the status of these satellites is available from the National Oceanic and Atmospheric Administration (NOAA) Office of Satellite Operations (OSO) at the website http://www.oso.noaa.gov/goesstatus/.

When it was decommissioned, each satellite was boosted into the "graveyard" or disposal orbit, at least 300 km above the geostationary ring. After being decommissioned, each satellite has drifted slowly westward in the disposal orbit, at a rate between four and 5 degrees per day. At these drift rates, each satellite returns to view every 80 to 90 days, providing sequential opportunities for observation and temporal analysis.

Some current orbital parameters for GOES 8 through 12 are listed in Table 2. The inclinations vary, but the main difference between the satellites' orbits is the larger eccentricity of the orbit of GOES 10.

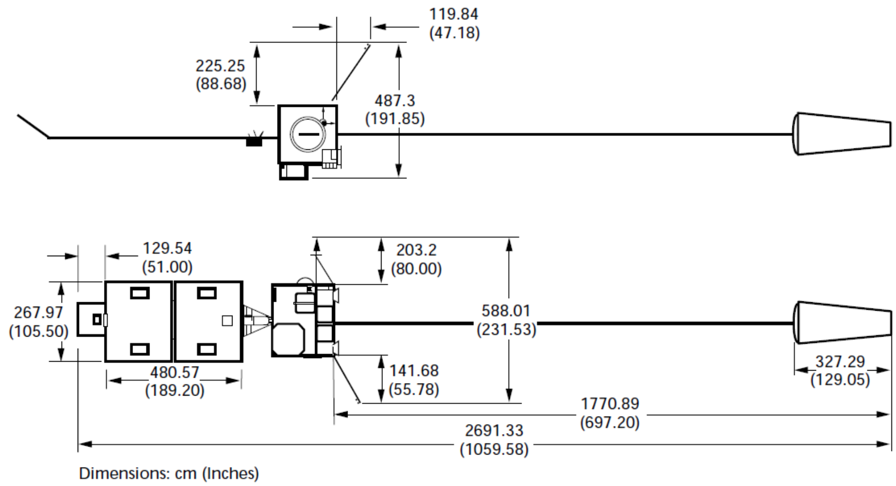

Fig. 1. Outline and dimensions of GOES, from *The GOES I-M Databook* [5]

Table 1. GOES launch and decommission dates

Satellite Name	*Catalog Number*	*International Designator*	*Launch Date*	*Decommission Date*
GOES 8	23051	1994-022A	1994-04-13	2004-05-05
GOES 9	23581	1995-025A	1995-05-23	2007-06-15
GOES 10	24786	1997-019A	1997-04-25	2009-12-02
GOES 11	26352	2000-022A	2000-05-03	2011-12-16
GOES 12	26871	2001-031A	2001-07-03	2013-08-16

Table 2. Orbital parameters of GOES 8 through 12

Satellite Name	*Inclination*	*Mean Motion (rev/day)*	*Eccentricity*
GOES 8	9.9°	0.989	0.00060
GOES 9	9.4°	0.988	0.00072
GOES 10	7.7°	0.991	0.00307
GOES 11	2.9°	0.990	0.00067
GOES 12	4.4°	0.991	0.00063

3. METHODS

The telescope used in the observations is the Oceanit-designed MStar, a modified Cassegrain telescope optimized for satellite tracking with a wide, flat field of view. It has a 0.4-m (16”) aperture at f/4.7. The MStar is housed in a dome near sea level in the Maui Research and Technology Center (MRTC) in Kihei, Hawaii. Its camera is the Apogee Alta U47, with 1024 by 1024 pixels. On the MStar, the camera’s field of view is 0.4 degrees wide, with a plate scale of 1.43 arc-seconds per pixel at full resolution. In this investigation, the images are typically binned for faster sampling cadence, so the plate scale is doubled. The images are acquired through a Johnson R filter.

The MStar sits on a German equatorial mount controlled by Software Bisque’s TheSky6 software. TheSky6 enables the telescope to track at the angular rate of satellite motion by propagating the orbit for each satellite from a two-line element set (TLE) downloaded from www.space-track.org.

As the satellite is tracked, the camera continuously acquires images. The exposure and sampling rate are adjusted to accommodate the expected satellite brightness and rotation period. With a binned image and 1.5-s exposures, the sampling cadence is once per 3.5 seconds. The sampling period is 5 seconds for full resolution images with 2-s exposure. The span of observations depends upon the expected period, and can extend to several hours. Fig. 2 shows the image acquisition site, the MStar in its dome, and a typical image from the observations.

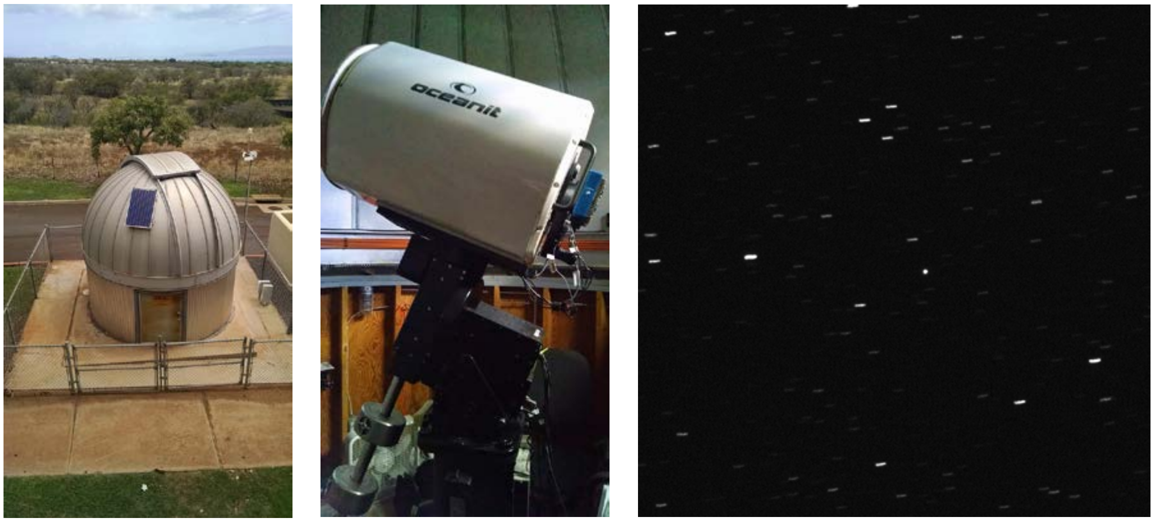

Fig. 2. The MRTC dome (left), the MStar in the dome (center) and a 2-s image of GOES 11 (right)

4. ANALYSIS

The images are calibrated with dark subtraction, and then a synthesized background image is subtracted from each frame. The details of the construction of the background image, which accounts for ambient sky and clouds, have been described previously [6]. The star streaks in the reduced image are detected and matched to a star catalog that is a hybrid of the Tycho-2 catalog and the USNO B 1.0 catalog from the United States Naval Observatory. The magnitudes of the matched stars calibrate the flux levels in each frame to provide the apparent R magnitude of the satellite in that frame. The timestamp for each measurement is at the midpoint of the exposure. The apparent R magnitude as a function of time forms the light curve, which is then analyzed to determine the rotation period of the satellite.

The analyses implemented here to determine the satellites' rotation periods are similar to those used by Scott and Wallace [7] in their small-telescope observations of Telstar 401 and Anik D1. A Fast Fourier Transform of the light curve, implemented in MATLAB, yields a set of candidate rotation periods. An autocorrelation, also in MATLAB, is optionally performed to help identify longer periods. Then the light curve is folded on the candidate periods in a process referred to as "epoch folding" in the astronomy community [8]. The epoch folding is implemented in Microsoft Excel in a way that allows incremental variations in the period over a wide range of values [9]. Minimization of the scatter in the magnitudes at each phase of the period identifies the true rotation period.

The periods that are identified here are the synodic rotation periods, not the sidereal rotation periods. Hall [10] has shown that the synodic and sidereal rotation rates differ by the rate of change in the phase angle bisector. For relatively fast rotations at GEO, the two rates are not appreciably different. For slower rotations, the neglect of the phase angle bisector's rate of change will introduce error.

5. RESULTS AND DISCUSSION

5.1 Rotational Differences among the Satellites

The unexpected result of these observations is the difference in the light curves. Fig. 3 shows the light curves of GOES 8 and GOES 9, simultaneously observed on an evening when both satellites appeared in the same field of view. The curves are plotted on the same time axis. Clearly the rotation period of GOES 8 is much shorter. Both satellites had been inactive for years at the time of this observation, and so the expectation was that both would have stabilized to a similar rotation state. The observations reveal very different rotational behavior.

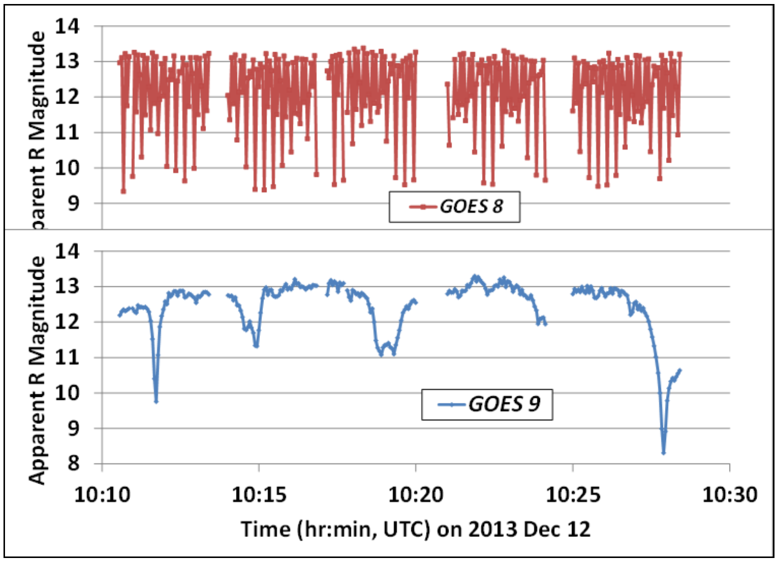

Fig. 3 Light curves of GOES 8 and GOES 9 observed simultaneously on 12 Dec 2013

The differences between GOES 8 and GOES 9 represent the two groups into which this block of satellites can be categorized based upon the nature of their rotations. GOES 8 and GOES 10 fall into the first group. These satellites have short rotation periods, on the order of tens of seconds, and their light curves have been fairly repeatable in these observations. Their rotation periods can be determined with some certainty.

GOES 9, GOES 11, and GOES 12 fall into the second group. Their rotational behavior appears to be more complex, and the periods are on the order of minutes or tens of minutes. Their light curves may be better analyzed with a technique such as wavelet analysis, which is beyond the scope of the present work. Nevertheless, their light curves are presented and analyzed here.

5.2 GOES 8

GOES 8 was observed on three separate occasions between December 2013 and late July 2014. The conditions of each observation, and the resulting periods, are listed in Table 3.

Table 3. Observation conditions and rotation periods of GOES 8

Date (UTC)	*Time (hr:min, UTC)*	*Azimuth/Elevation*	*Solar Phase Angle*	*Period*
2013-12-12	10:10 – 10:28	224°/59°	34° - 30°	16.83 s
2014-02-27	14:56 – 16:07	254°/54°	22° - 39°	16.48 s
2014-07-25	8:21 – 8:40	241°/28°	13° - 9°	75.66 s

The light curves for GOES 8 are simple and lend themselves easily to determination by epoch folding. The folded light curves obtained on each of observation dates in Table 3 are shown in Fig. 4. Regardless of the angle of view, the rotation of GOES 8 is characterized by two peaks in brightness, one stronger than the other.

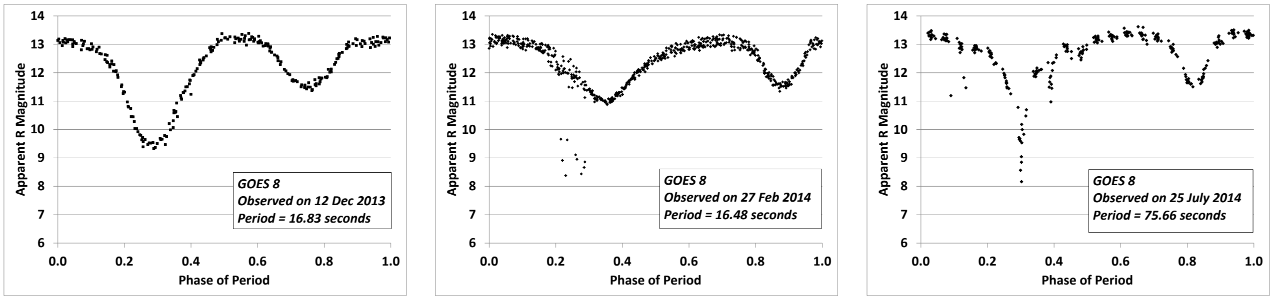

Fig. 4. Folded light curves from observations of GOES 8

5.3 GOES 10

Like GOES 8, GOES 10 was also observed successfully on three occasions. The conditions of each observation and the resulting periods are listed in Table 4.

Table 4. Observation conditions and rotation periods of GOES 10

Date (UTC)	*Time (hr:min, UTC)*	*Azimuth/Elevation*	*Solar Phase Angle*	*Period*
2014-02-28	5:29 – 6:27	109°/50°	25° - 40°	31.1 s
2014-03-19	15:04 – 15:28	256°/34°	14° - 20°	32.5 s
2014-08-28	8:21 – 8:40	171°/57°	22° - 26°	26.2 s

The folded light curves for GOES 10 are shown in Fig. 5. Each rotation is characterized by 4 peaks in brightness, in contrast with the two peaks of each rotation of GOES 8. The relative magnitudes of the peaks change with viewing angle and illumination condition. In the first two observations, the periods are nearly double the periods in the first two observations of GOES 8, even though they are clearly not a simple harmonic of the GOES 8 periods.

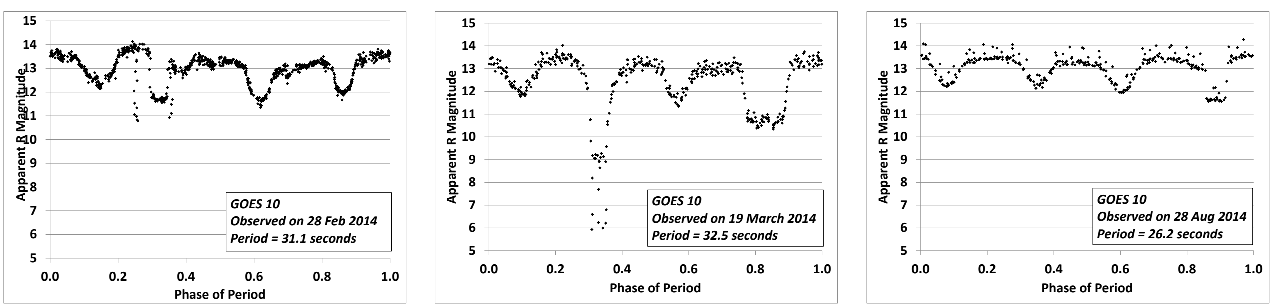

Fig. 5. Folded light curves from observations of GOES 10

One explanation for the difference between the GOES 8 and GOES 10 light curves may lie in the changes experienced by GOES 10 since its decommissioning. NASA's *Orbital Debris Quarterly News* [11] reported an anomalous change in orbit of the inactive satellite, whose perigee suddenly decreased by 20 km on 5 September 2011. A second abrupt change in the orbit in early 2012 is revealed by examination of its TLEs. The eccentricity of the orbit increased sharply as a result of the 2012 event. The mean motion and the eccentricity from the TLEs are plotted in Fig. 6.

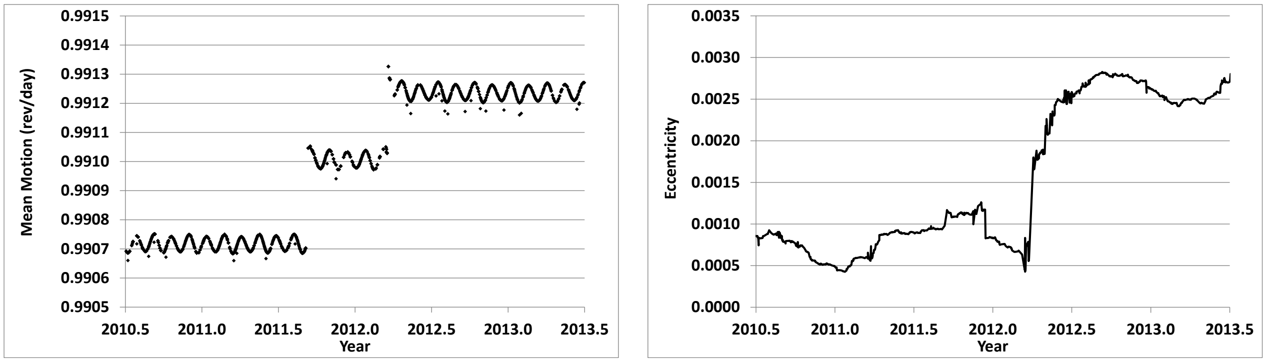

Fig. 6. Abrupt changes in mean motion (left) and orbital eccentricity (right) experienced by GOES 10

5.4 GOES 9

GOES 9 was observed for almost two hours on 4 July 2014. The conditions of the observation are listed in Table 5, and a 70-minute portion of the light curve is shown in Fig. 7. A strong glint at 14:02 appears in only one frame. Folding the curve on a period of 9.1 minutes produces two peaks in brightness, like the rotations of GOES 8, though the folds are not well-matched. A longer period of approximately 22.7 minutes is a slightly better fit to the data, but only 3 periods are covered by this span of data. The folded light curves for both periods are shown in Fig. 8.

Table 5. Observation and rotation period of GOES 9

Date (UTC)	*Time (hr:min, UTC)*	*Azimuth/Elevation*	*Solar Phase Angle*	*Period*
2014-07-04	13:11 – 15:00	215°/49°	19° - 43°	22.7 min

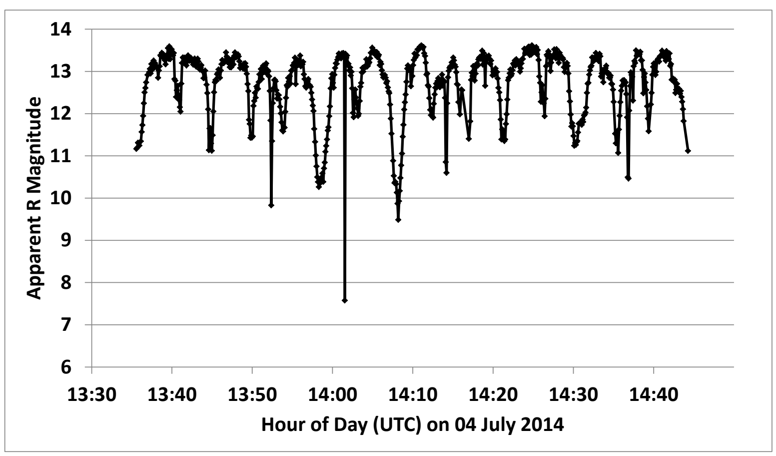

Fig. 7. A portion of the GOES 9 light curve

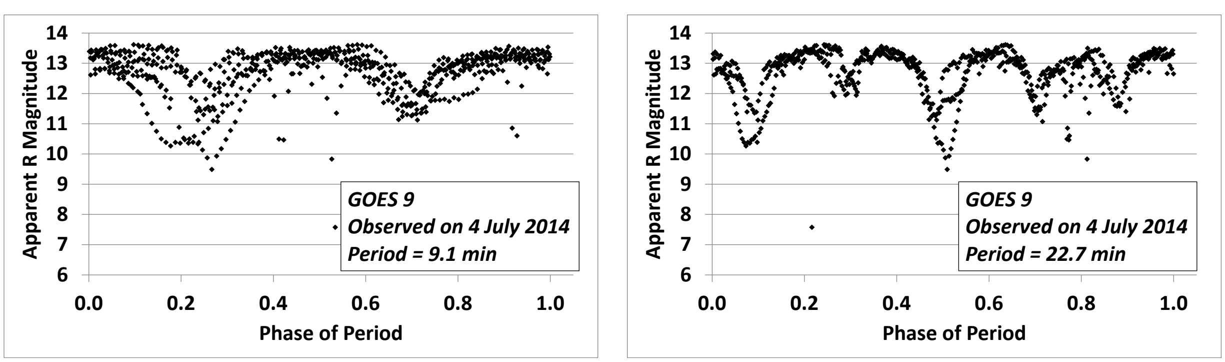

Fig. 8. GOES 9 light curve folded on 9.1-min period (left) and 22.7-min period (right)

5.5 GOES 11

GOES 11 was observed for more than 3 hours, with some gaps. For consistent comparison with GOES 9, a 70-minute span of data is analyzed here. Table 6 describes the observation and the period that results from epoch folding of the light curve. Both the light curve and the folded light curve are shown in Fig. 9.

Table 6. Observation and rotation period of GOES 11

Date (UTC)	*Time (hr:min, UTC)*	*Azimuth/Elevation*	*Solar Phase Angle*	*Period*
2014.08.15	6:35 – 7:45	119°/42°	20° - 8°	20.9 min

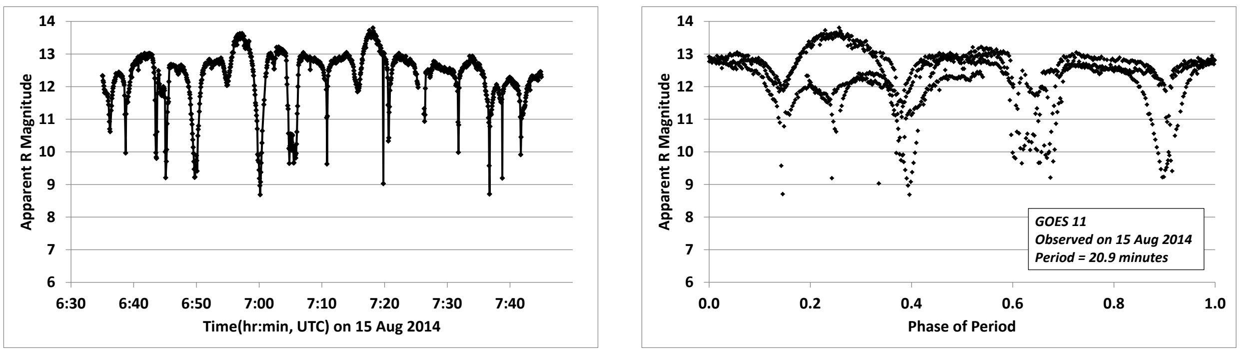

Fig. 9. The light curve (left) and the folded light curve (right) from observation of GOES 11

5.6 GOES 12

GOES 12 was observed on three different occasions, summarized in Table 7. Only on 28 August is a 70-minute span of data available; the other observations are shorter.

Table 7. Observations of GOES 12 with period of best fold of each light curve

Date (UTC)	*Time (hr:min, UTC)*	*Azimuth/Elevation*	*Solar Phase Angle*	*Period**
2014-03-05	14:51 – 15:49	199°/66°	56° - 71°	9.75 min
2014-05-22	9:09 – 9:46	117°/42°	28° - 35°	11.4 min
2014-08-28	8:46 – 10:04	190°/61°	30° - 11°	13.8 min

***Period of best fold may not be actual rotation period.**

The use of epoch folding is relatively unsuccessful in the determination of the rotation periods for GOES 12. For none of the observations in Table 7 do the folded light curves align well. Part of the mismatch may be due to the evolution of the synodic period over the large timespan, but apparently there are also time-varying periods and rotation about more than one axis. The best folds are shown alongside their original light curves in Fig. 10 through Fig. 12.

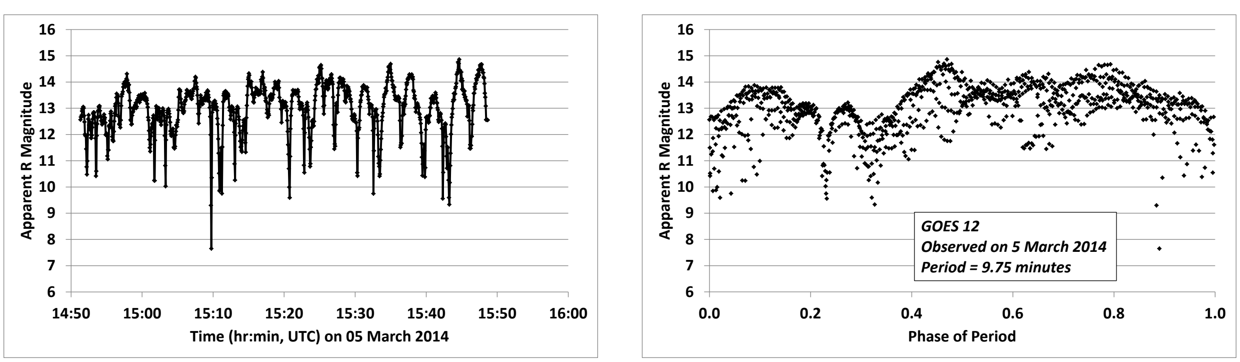

Fig. 10. Light curve (left) and folded light curve (right) from observation of GOES 12 on 5 March 2014.

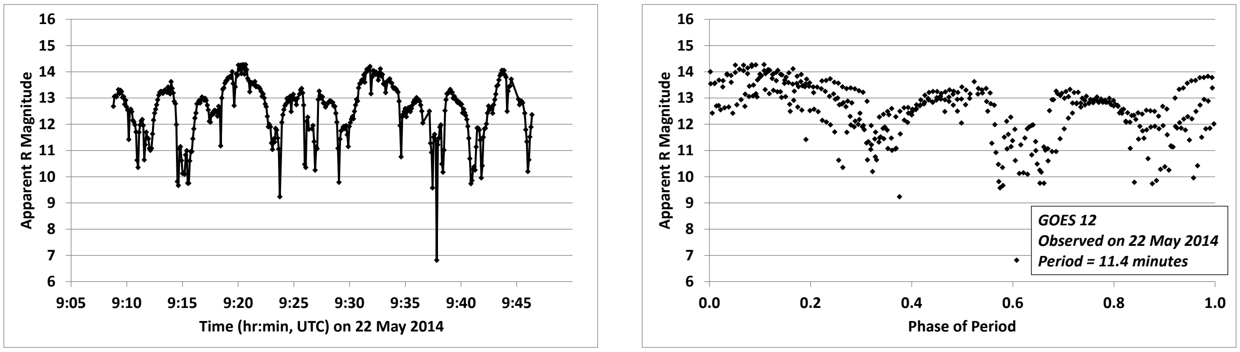

Fig. 11. Light curve (left) and folded light curve (right) from observation of GOES 12 on 22 May 2014.

In Fig. 12, the folded curve is for the timespan from 8:45 UTC to 9:46 UTC. The data above 9:50 UTC were included in the FFT analysis, but have been removed from the graph in order to improve the visibility of the fold.

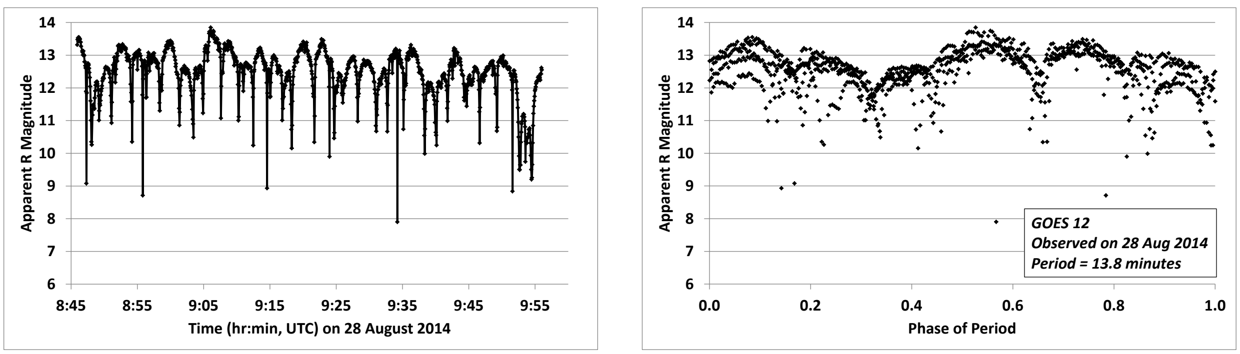

Fig. 12. Light curve (left) and folded light curve (right) from observation of GOES 12 on 28 Aug 2014.

6. CONCLUSIONS

The satellites known as GOES 8 through GOES 12, a decommissioned subset of the GOES constellation, present a useful test case for the study of the dynamics of inactive GEO satellites as a function of time. Of the same build, and decommissioned sequentially over a 10-year period, the inactive satellites were observed through a small telescope over several months as they drifted into view over Maui, and the rotation period for each satellite was determined from its light curve.

The observed rotation periods range from approximately 16 seconds to more than 20 minutes, and the satellites fall into two groups, according to their rotation behavior. Both GOES 8 and GOES 10 exhibit simple rotations whose periods are tens of seconds. GOES 9, GOES 11, and GOES 12 exhibit more complicated, apparently multi-axial tumbling, whose periods are minutes or tens of minutes. The periods of rotation for the satellites in the latter group were not conclusively determined by the epoch folding method.

Even though the satellites are of the same build, their light curves differ. On-orbit changes to some of the satellites (notably GOES 10) may be responsible for some of the differences. Continued observation is recommended in order to characterize evolving dynamics, and analysis of the light curves with another method (such as wavelet analysis) is also recommended in order to determine multi-axial and evolving angular velocities.

7. ACKNOWLEDGMENTS

John Tsui of the National Oceanic and Atmospheric Administration (NOAA) provided useful information regarding the end-of-life configurations of the GOESs.

Discussion with Doyle Hall of Boeing provided useful insight into the shortcomings of the FFT in determining the rotation period.

The use of the MStar telescope was made possible through a cooperative agreement between Oceanit and United States Air Force Space Command SMC/SYET.

8. REFERENCES

1. Wormnes, K., et al., "ESA Technologies for Space Debris Remediation," 6th European Conference on Space Debris, Darmstadt, Germany, 22-25 April 2013.
2. ESA's Clean Space website, http://www.esa.int/Our_Activities/Space_Engineering/Clean_Space, accessed on 6 Sept. 2014.
3. DARPA's Phoenix website, http://www.darpa.mil/Our_Work/TTO/Programs/Phoenix.aspx, accessed on 6 Sept 2013.
4. Weeden, B., Chow, T., Samson, V., and Lukaszczyk, A., "International Perspectives on On-orbit Satellite Servicing and Active Debris Removal and Recommendations for a Sustainable Path Forward", IAC-13.E3.4.7, 64th International Astronautical Congress, Beijing, China, September 23-27, 2013.
5. *GOES I-M Databook*, Rev. 1, 31 August 1996, http://rsd.gsfc.nasa.gov/goes/text/databook/databook.pdf, downloaded on 7 Nov. 2013.
6. Cognion, R., "Large phase angle observations of GEO satellites," *Proc. SPIE* 8739, Sensors and Systems for Space Applications VI, 87390K (21 May 2013).
7. Scott, L., and Wallace, B., "Satellite characterization using small aperture instruments at DRDC Ottawa," *Proceedings of the Advanced Maui Optical and Space Surveillance Technologies Conference* [CD], Wailea, Hawaii (2008).
8. Leahy, D.A., et al., "On Searches for Pulsed Emission with Application to Four Globular Cluster X-Ray Sources: NGC 1851, 6441, 6624, and 6712," The Astrophysical Journal, Vol. 266, pp 160-170, 1 March 1983.
9. "How to Fold a Light Curve using Excel," http://talk.planethunters.org/discussions/DPH100suj9, accessed on 2 Sept. 2014.
10. Hall, D., et al., "AMOS Observations of NASA's IMAGE Satellite," *Proceedings of the Advanced Maui Optical and Space Surveillance Technologies Conference* [CD], Wailea, Hawaii (2006).
11. "Two Derelict NOAA Satellites Experience Anomalous Events," *Orbital Debris Quarterly Newsletter*, edited by Shoots, D., Houston, TX: NASA, Vol. 16, No. 1, January 2012.